Tree Physiology 00, 1–13
https://doi.org/10.1093/treephys/tpad083

Research paper

# Moisture stress limits radial mixing of non-structural carbohydrates in sapwood of trembling aspen

Drew M. P. Peltier[1,4], Phiyen Nguyen[2], Chris Ebert[1], George W. Koch[1,2], Edward A. G. Schuur[1,2] and Kiona Ogle[1,2,3]

[1]Center for Ecosystem Science and Society, Northern Arizona University, PO Box 5620, Flagstaff, AZ 86011, USA; [2]Department of Biological Sciences, Northern Arizona University, PO Box 5640, Flagstaff, AZ 86011, USA; [3]School of Informatics, Computing, and Cyber Systems, Northern Arizona University, PO Box 5693, AZ 86011, USA; [4]Corresponding author (dmp334@nau.edu)

Received January 23, 2023; Accepted June 27, 2023; handling Editor Lucas Cernusak

**Dynamics in non-structural carbohydrate (NSC) pools may underlie observed drought legacies in tree growth. We assessed how aridity influences the dynamics of different-aged NSC pools in tree sapwood at two sites with differing climate conditions ('wet' vs 'dry'), which also experienced widespread regional drought 5 years earlier. We used an incubation method to measure the radiocarbon ($\Delta^{14}C$) in $CO_2$ respired from *Populus tremuloides Michx.* (aspen) tree rings to evaluate NSC storage and mixing patterns, coupled with measurements of NSC (soluble sugars and starch) concentrations and respired $\delta^{13}C$-$CO_2$. At a wet site, $CO_2$ respired from rings formed during 1962–67 was only ~11 years old, suggesting deep sapwood mixing of NSCs as starch. At a dry site, the total NSC was about one-third of wet-site totals, maximum ages in deep rings were lower and ages more rapidly increased in shallow rings and then plateaued. These results suggest historically shallower mixing and/or relatively higher consumption of NSCs under dry conditions. Both sites, however, had similar aged NSC (<1 year) in the most recent six rings, indicative of deep radial mixing following relatively wet conditions during the sampling year. We suggest that the significant differences in NSC mixing among sites are driven by moisture stress, where aridity reduces NSC reserves and restricts the depth of radial mixing. However, dynamic climate conditions in the south-western USA resulted in more complex radial patterns of sapwood NSC age than previously described. We suggest a novel conceptual framework to understand how moisture variability might influence the dynamics of NSC mixing in the sapwood.**

***Keywords***: bomb spike, drought legacy, NSC, radiocarbon.

## Introduction

The pools and fluxes of non-structural carbohydrates (NSCs; soluble sugars and insoluble starch) drive tree physiological processes from growth and reproduction (e.g., Dietze et al. 2014, Palacio et al. 2014) to stress tolerance and drought mortality (Kobe 1997, Sala et al. 2012, O'Brien et al. 2014). The NSC storage in trees can also be large: total sapwood NSC can represent up to four times the carbon required to rebuild the canopy in some deciduous species (Hoch et al. 2003). Characterization of whole-tree NSC pools, while challenging, has shown stemwood and branches to be major organs of NSC storage, with concentrations that vary seasonally (Barbaroux and Bréda 2002, Furze et al. 2018*a*). Within the stem, radial variation in NSC reflects higher concentrations in young sapwood, which also exhibits the largest seasonality in NSC concentrations (Barbaroux and Bréda 2002, Hoch et al. 2003, Richardson et al. 2013, Furze et al. 2018*b*). Potentially of interest is how storage and mixing—the radial movement of sapwood NSC—may respond to climate warming and drought, given that changes in such physiological processes, especially in foundation tree species (e.g., *Populus tremuloides* Michx.; Cole et al. 2010), could have cascading impacts on forested ecosystems (Ellison et al. 2005).

Numerous experiments have quantified the NSC status prior to drought-induced tree mortality, providing information on the changes in NSC pools under drought (e.g.,

Anderegg et al. 2012, Adams et al. 2013, Dickman et al. 2015). While NSC pools can decrease during long-term and severe drought (though, interconversions may increase soluble fractions; Dickman et al. 2015, He et al. 2020), trees often fail to completely exhaust NSC pools during drought experiments, suggesting the inability to mobilize or transport sugars under extreme hydraulic stress or death before complete remobilization (e.g., Adams et al. 2017). In the south-western USA, short-term sink limitation may play a role in driving NSC dynamics in the canopies of *P. tremuloides* (aspen), but these trees show responses reflective of NSC depletion at drier sites (Peltier et al. 2020). While hydraulics are a major focus of drought impacts, NSCs may play a role in recovery from hydraulic damage, particularly under active refilling where NSCs are the likely source of osmolytes (Bloemen et al. 2016, Savi et al. 2016, Yoshimura et al. 2016) or xylem regrowth (Trugman et al. 2018). However, the question of what percent of whole-tree NSC is potentially available for respiratory or osmoregulatory needs under drought stress is essentially unresolved (Sala et al. 2010). Moreover, perhaps, the availability or ability to transport deep stem NSC may be constrained by moisture stress.

Characterization of the age (time since fixation) of NSC has the potential to improve our understanding of reserve cycling and dynamics under drought, but the application of these methods has mostly been limited to relatively mesic environments. Radiocarbon ($\Delta^{14}C$) dating of NSC fixation date ('age'), according to the bomb spike (Levin and Kromer 2004), suggests the existence of multiple NSC 'pools' characterized by different ages and cycling rates (Carbone et al. 2013, Richardson et al. 2015, Trumbore et al. 2015). The NSCs are added to these pools (via mixing of new photosynthate into existing stores in older tissues) and used (following remobilization) over multiple years, and drought stress might affect the age of NSC pools. For example, trees with relatively young NSC pools might be more vulnerable to transient disturbance, as they turn over NSC, on average, more rapidly than trees with older NSC pools. Sapwood $\Delta^{14}C$ studies suggest that young, recently fixed NSCs observed in the most recent three to five rings match the ages of respired $CO_2$, while older NSC stores in deeper rings are drawn upon only during severe stress (Carbone et al. 2013, Muhr et al. 2018). Such studies are extremely limited, however, and there are still major uncertainties about the functioning of and climatic controls on tree NSC storage, allocation and age (Furze et al. 2018*b*). In particular, the generality of these results across species (i.e., wood anatomies) or sites remains unclear, and it is unknown how aridity may influence these processes (but, see Trumbore et al. 2015). Thus, while many investigators have focused on NSCs in drought-related tree mortality, it is unclear how varying aridity may influence the NSC age or the relative sizes of different-aged NSC pools.

To understand how moisture stress may influence NSC mixing and utilization, we evaluated the size and age of NSC pools in sapwood and bark of quaking aspen (*P. tremuloides*) occurring in two natural stands of varying aridity, where recent drought stress significantly reduced the mean ring width (RW) at the drier site. While infrequently characterized, living bark tissue (hereafter, 'bark') in aspen represents a major storage organ (Landhäusser and Lieffers 2003, Richardson et al. 2015, Wiley et al. 2019). Here, we measured the $\Delta^{14}C$ and $\delta^{13}C$ of respired $CO_2$ collected from aspen sapwood rings and bark using a previously validated incubation method (Peltier et al. 2023) and simultaneously quantified extractable NSC pool sizes (soluble sugars and starch). We addressed two broad questions: (Q1) How do extractable NSC pool sizes differ between a wet and dry site following recent drought? (Q2) Do respired $CO_2$ age or their radial patterns differ between wet and dry sites, indicating different reliance on old versus recently fixed NSC? With respect to Q1, we hypothesize that (hypothesis 1 (H1)) trees at a dry site store less NSC relative to trees at a wet site. With respect to Q2, we hypothesize that (hypothesis 2 (H2)) trees at a dry site exhibit shallower mixing (as evidenced by 'older' respired NSC in sapwood rings). Addressing these questions and hypotheses led us to integrate the roles of inter-annual variability and site-level differences in moisture into a novel conceptual framework describing the influence of aridity and climate variability on NSC mixing and consumption. Sampling design was necessarily limited by sample costs, but we emphasize the novelty of this study, the unique data and hypotheses generated for future studies of tree carbon cycling.

## Materials and methods

### *Study sites*

We selected two sites (near Tres Piedras, NM, and Junction, UT; Table 1, Figure S1 available as Supplementary data at *Tree Physiology* Online) established in 2016 as part of another study in the south-western USA (Peltier et al. 2020). For that study, 15 dominant aspen trees per site were cored (summer 2017), cross-dated and RWs were measured following standard methods (Fritts and Swetnam 1989). Bulk wood density (WD) (g per $m^3$) was measured via water displacement on a scale. The two study sites (hereafter, 'wet site' and 'dry site') represent moisture extremes (Table 1; Figures S1 and S2 available as Supplementary data at *Tree Physiology* Online), and we measured NSC, $\delta^{13}C$ and $\Delta^{14}C$ in trees from both sites (Table 2). This region also experienced widespread drought in 2011–12 (Weiss et al. 2012), an event which differentially affected these two sites: wet-site trees are highly vigorous, with little evidence of drought impacts in RWs (Table 1) or appearance (Figure S1 available as Supplementary data at *Tree Physiology* Online), while dry-site trees showed clear RW depression following the drought (Table 1), with clear evidence of recent canopy dieback in some study trees and across the site (Figure S1 available as Supplementary data at *Tree Physiology* Online). Climate conditions in the weeks prior to sampling at each site may have

Table 1. Two sites were visited multiple times to collect tree cores for NSC and for $\delta^{13}C$ and $\Delta^{14}C$ incubations in the summer of 2017. Site names, locations and characteristics are noted. Mean (growth) sensitivity was determined from the tree RW measurements and was calculated with COFECHA (Holmes 1983). Mean ± SD of RWs are also reported for 'young' and 'old' rings. Mean annual precipitation (MAP) and mean annual temperature (MAT) covers the period 1986–2017 (data obtained from PRISM climate group, http://prism.oregonstate.edu). Leaf $^{13}C$ was measured by the Colorado Plateau Stable Isotope Laboratory on canopy leaves from five trees at each site collected in summer 2016 on 6/28 and 8/25 (dry site) and 6/16 and 8/18 (wet site), and data presented are means. Two leaf samples were lost at the wet site in the spring sample (6/16). Site visit dates and sample sizes are given in Table 2. Mean DBH and height (Ht) of study trees are also reported.

| Site | State | Coordinates (decimal degrees) | Mean sensitivity[1] | RW pre-2012 (mm) | RW 2012-17 (mm) | MAP (mm per year) | MAT (°C) | Elevation (m.a.s.l.) | Aspect | Leaf $^{13}C$ (‰) Spr '16, Fall '16 | DBH (cm) | Ht (m) |
|---|---|---|---|---|---|---|---|---|---|---|---|---|
| Dry | NM | 36.63, −106.17 | 0.433 | 1.48 ± 0.73 | 0.64 ± 0.34 | 550.6 | 4.84 | 2847 | South | −26.1, −26.9 | 21.1 ± 5.5 | 9.9 ± 1.5 |
| Wet | UT | 38.25, −112.42 | 0.258 | 1.68 ± 0.64 | 1.86 ± 0.60 | 842.3 | 3.84 | 2946 | None | −26.8, −27.5 | 37.7 ± 13.0 | 12.8 ± 1.8 |

[1]An index commonly used in dendrochronology to describe the usefulness of trees at a given site for climate reconstruction, where values near 0.7 are considered to be very high (large year-to-year variability in RWs), typical of conifers at a dry site in the south-western USA, and values around 0.2 are considered to be fairly low, indicative of 'complacent' trees (comparatively little year-to-year variability in RWs).

influenced our results, and we acknowledge that we did not control for this, though our $^{14}C$ data (see Results) suggest that the relative influence should be small as NSC could be quite old. Conditions in the sampling year were similar to long-term climate averages. Though we did not precisely estimate tree ages, most trees were ∼40–80 years old, and some were >100 years old. We collected similar data from four additional sites spanning the aridity gradient of the focal (wet and dry) sites (Table S1 available as Supplementary data at *Tree Physiology* Online), but we primarily focus on the focal sites. Focal site soils had similar fractions >2 mm (wet: 37.7%, dry: 31.6%) and C:N ratios (18.0 and 17.7, respectively) (analyzed by Forest Inventory and Analysis program; Gillespie 1999).

### *Physiological tree cores*

In 2017, trees were cored at breast height using a 12-mm diameter Mattson increment borer (Haglöf, Långsele, Sweden). Some dry-site trees were cored for NSC and $^{13}C$ twice during the season (Table 2). Snow prevented spring sampling at the wet site (Table 2). Thus, '$^{14}C$ cores' were only collected during or after leaf senescence when NSC storage is near seasonal maxima (Furze et al. 2018*b*). To reduce contamination, the outer surface of the bark was removed when coring. We experimented with sanitizing the borer with ethanol in the field, which proved too difficult to completely evaporate, and we abandoned this after $\Delta^{14}C$ measurements in pilot samples showed ethanol contamination. Thus, the borer was thoroughly cleaned with ethanol between site visits, and no oil was used. Cores were sealed in ziploc bags (NSC and $\delta^{13}C$ cores) or glass jars ($^{14}C$ cores) and were transported on ice to Flagstaff, AZ, USA. Prior to incubation for $\Delta^{14}C$ (see $\Delta^{14}C$ incubations section), to accommodate multi-day field trips with different transport times, all cores were kept on ice for 48 h (Figure 1, first panel). After this time, cores for NSC quantification ('NSC cores') were frozen at ∼−20 °C.

### *Non-structural carbohydrate quantification*

The NSC cores were sectioned (see $\Delta^{14}C$ incubations), dried in a drying oven at 60 °C for 72 h and ground to a fine powder (Retsch MM200 ball mill, Haan, Germany); ∼0.05 g was analyzed for NSC concentrations following the Chow–Landhäusser method (Chow and Landhäusser 2004, Quentin et al. 2015, Landhäusser et al. 2018), except we did not microwave NSC samples prior to drying, given our analysis occurred prior to Landhäusser et al.'s (2018) recommendation to microwave. In combination with the 48-h lag (designed to assure we quantified the same NSC pools respired in isotopic incubations), our NSC concentrations are likely somewhat lower than the 'true' values (i.e., if microwaved after coring). Briefly, soluble sugars were extracted in three rounds of 70 °C ethanol and were quantified using a colorimetric phenol-sulfuric acid (>95%) reaction, with absorbance read at 490 nm on a

Table 2. Sample sizes for the two focal sites (see Table 1) with sampling dates in 2017, where a unique sample is a section of multiple rings, from either the bark or sapwood, analyzed together for one of NSC, $\delta^{13}C$ or $\Delta^{14}C$. We also note the number of trees represented by the sapwood and bark samples.

| | | Spring–summer | | Fall–winter | |
|---|---|---|---|---|---|
| Variable | Unit | Dry | Wet | Dry | Wet |
| NSC | Sapwood | 25 | — | 28 | 72 |
| | Bark | — | — | 7 | 6 |
| | Trees | 2 | — | 5 | 6 |
| Dates sampled | | 4/21, 5/26 | — | 11/10 | 9/24, 12/16 |
| $\delta^{13}C$ | Sapwood | 12[1] | — | 36 | 49 |
| | Bark | — | — | 14 | 13 |
| | Trees | 4 | — | 5 | 6 |
| Dates sampled | | 4/21, 5/26 | — | 11/10 | 9/24, 12/16 |
| $\Delta^{14}C$ | Sapwood | — | — | 21 | 22 |
| | Bark | — | — | 9 | 6 |
| | Trees | — | — | 5 | 5 |
| Dates sampled | | — | — | 11/10 | 9/24, 12/16 |

[1]Only measured in 'young rings' (rings 1–6).

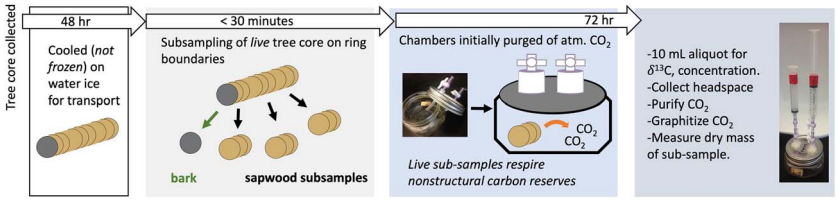


Figure 1. Overview of key steps in the incubation method for collecting respired $CO_2$ from live tree-ring samples for measurement of $\Delta^{14}C$ of NSC. More details are provided in Peltier et al. (2023). Details of $\delta^{13}C$ concentration correction are described in Table S1 available as Supplementary data at *Tree Physiology* Online.

UV–Vis spectrophotometer with a 96-well microplate reader (Synergy H1, Bio-Tek Instruments, Winooski, VT, USA). Starch pellets were solubilized in sodium hydroxide (30 min), digested with an $\alpha$-amylase and amyloglucosidase (Sigma-Aldrich, St. Louis, Missouri, USA) mixture for 48 h at 50 °C and quantified (glucose-equivalents) using a 45-min colorimetric reaction with PGO enzyme (Sigma-Aldrich) terminated with 75% sulfuric acid. Absorbance was read on the UV–Vis spectrophotometer (525 nm). Concentrations were calculated from simultaneously generated glucose standard curves. Standard curve slopes and intercepts were closely monitored for consistency, with runs being repeated as necessary. An in-house standard (homogenized ground aspen branches stored in a frozen desiccator) was measured per 12 samples. To estimate NSC consumption during incubations, we measured NSC on 14 previously incubated samples (see below).

### *Sapwood NSC pools*

Because RWs are likely to be larger at the wetter site, NSC concentrations may not fully capture the differences in NSC that are available to trees. Thus, to compare NSC storage in sapwood between sites, while accounting for each tree's WD and RWs, we scaled NSC concentrations (mg glucose equivalents per g dry weight) to a quantity approximating volume-specific sapwood NSC storage (mg glucose equivalents per ring) in 1-cm thick cross-sections of each ring. We evaluated total NSC storage only in the fall since NSC data are not available for the spring at the wet site (Table 2). First, ring-wise diameter at breast height (DBH) was estimated as:

$$DBH_{r,t} = DBH_{1,t} - 2\sum_{i=1}^{r-1} RW_{i,t} \text{ for } r = 2, 3, \ldots, \quad (1)$$

where $DBH_{r,t}$ is bole diameter when ring $r$ was the outermost ring for tree $t$, where $r$ = 1, 2, 3, ..., corresponds to rings formed in 2017, 2016, 2015, ..., respectively (e.g., $DBH_{1,t}$ is the bole diameter in 2017). The $RW_{r,t}$ is the width for ring $r$ and tree $t$. This assumes (i) RW is constant within each ring across the tree circumference and (ii) a circular bole (fairly appropriate for aspen). The RWs were measured on two cores from different sides of the tree, and we averaged the two RWs to define $RW_{r,t}$.

Then, total NSC pool size in each ring was estimated as the cross-sectional area of a given ring (quantity inside brackets, [...], in Eq. (2)), multiplied by the NSC concentration (soluble

sugars plus starch in glucose equivalents) in subsample $s$ containing ring $r$, denoted $s(r)$, and by the average WD for that tree:

$$\text{PoolSize}_{r,t} = \left[\frac{\pi}{4}\left(\text{DBH}_{r,t}^2 - \text{DBH}_{r+1,t}^2\right)\right] \cdot \text{NSC}_{s(r),t} \cdot \text{WD}_t. \quad (2)$$

PoolSize estimates the mass of NSC stored in a 1-cm high cross-section of a given ring. Cumulative total NSC (sum of 6 ring increments up to 36 rings) was estimated for each tree by summing the $\text{PoolSize}_{r,t}$ across rings, with means subsequently calculated across trees within each site. Thus, even though the sampling of NSC was in pooled samples of multiple rings (below), this scaling was performed with a model in ring-wise fashion.

Analytical uncertainty in pool sizes introduced by the NSC and WD measurement error was estimated with Monte Carlo simulation to propagate errors, whereby we repeated these calculations (including among tree averages) for 1000 replicate (simulated) NSC concentrations and wood densities. Replicate concentrations were drawn from normal distributions, with means equal to the observed values and standard deviations (SDs) taken from the coefficients of variation (CVs) of repeat measurements of in-house standards (soluble sugars: CV = 19.5%; starch: CV = 16.1%, Figure S3 available as Supplementary data at *Tree Physiology* Online). A 5% CV was used for WD (likely conservative). Errors in pool sizes are reported as means of 1000 among-tree SDs from replicate calculations. We consider RW measurement error small (irrelevant) compared with NSC error, WD error and among tree variation.

### $\Delta^{14}C$ incubations

We used an incubation method to measure the $\Delta^{14}C$ of NSC, incubating live wood tissue in jars and capturing the respired $CO_2$ produced from the consumption of NSC (Figure 1). This method has been validated (Hilman et al. 2021, Peltier et al. 2023), though, as we conducted the sampling for this study a few years prior to those experiments, we only used a 3-day incubation period. We acknowledge this may have resulted in lower incubation yields (i.e., less consumption of NSC), but time series measurements in *P. tremuloides* have shown that $\Delta^{14}C$ of NSC is not strongly influenced by the incubation times, and so the $\Delta^{14}C$ from 3-day incubations should be similar to those obtained after 5 days (Peltier et al. 2023).

Preparations were made with living wood tissue (precluding drying or freezing), whereby 12-mm diameter cores were mounted horizontally on a vice with sanitized clamps, and a smooth surface was created using unlubricated razor blades (sanding the cores would have distributed material across ring boundaries). Referring to cross-dated cores collected on the same trees at roughly the same height when necessary, 12-mm cores were sliced at visually identified ring boundaries using a sharp razor blade, generating subsamples of 2–12 rings ('sections'). This process was relatively fast, as we simply confirmed that the ring sequence matched the dated core. Rings per section varied as we were limited by (i) the number of gas samples we could analyze quickly and (ii) the tissue mass required to obtain the target 0.5 mg of carbon for $\Delta^{14}C$ measurements. Thus, we opted to pool larger numbers of rings in certain sections, especially when the rings were extremely narrow (i.e., 2002–06), which avoided the error introduced by attempting to separate very narrow rings. We initially sought to mirror incubation ring sections in paired NSC measurements, which were sectioned using the same vice-mounting and surfacing method (no sanding), but later, we measured NSC as finely as possible (i.e., fewest rings per section, often two rings), somewhat opportunistically. For some trees (four at dry site and two at wet site), we sectioned the entire sapwood; otherwise, we sectioned at least 20 rings of sapwood. For NSC concentrations, we sectioned cores up to 36 rings in depth, where, for both sites, we sampled two trees at this deepest increment. Sapwood–heartwood boundaries were usually very obvious (indicated by dry, disintegrating heartwood bordered by dark stain typical of aspen). Cores requiring more sectioning time were prepared in a cold room (4.8 °C). We removed living bark tissue; see Table 2 for sample sizes.

Sapwood and bark sections were incubated using custom chambers: wide-mouth half pint (~236 ml) Ball jars (Broomfield, CO, USA) with modified lids. Similar methods are routinely applied in soil incubation studies, and can be used to obtain $CO_2$ for accelerator mass spectrometry (AMS) measurements of $\Delta^{14}C$ (e.g., Pegoraro et al. 2019). Here, two ports were installed per lid by using the screw on luer-lock fittings and valves sealed on the lid exterior with silicone (Figure 1). Chambers were initially flushed with $CO_2$-free air (Airgas, Radnor, PA, USA) through ports for 60 s and were shaken intermittently and then valves were shut; volume of flushing gas exceeded 10× total chamber volume. Preparation time never exceeded 40 minutes and was often much shorter. Jars were then incubated 72 h (3 days) at room temperature, which seemed to be a good compromise between $CO_2$ production and avoiding microbial decomposition. In later work, we have incubated 120 h (5 days), but this does not substantially impact the resulting $\Delta^{14}C$ (Peltier et al. 2023).

### Gas extraction, graphitization and $^{14}C$ analysis of respired $CO_2$

The $^{14}C$ samples were incubated following the procedure described above. Following incubation, gas was flushed from jars into 2-port 1-l tedlar gas bags (Keika Ventures, Chapel Hill, NC, USA) with compressed nitrogen (Figure 1). Bags were flushed three times between uses. Since 1 l is ~4× chamber volume, we assume the bag captures nearly all respired $CO_2$. The $\Delta^{13}C$ samples were collected via similar procedures as described for $\Delta^{14}C$ (but, on different cores), analyzed on a

Picarro G2201 Cavity Ring-Down Spectrophotometer (Santa Clara, CA, USA) and adjusted for mass (see Tables S2, Table S3, and Methods S1 available as Supplementary data at *Tree Physiology* Online). Gas for $\Delta^{14}C$ was pulled from the bags on a vacuum line, purified and $CO_2$ was converted to graphite (Lowe 1984, Vogel et al. 1984) for analysis at the W.M. Keck Carbon Cycle AMS facility (University of California, Irvine, CA, USA). To estimate contamination by atmosphere (leaks) and other sources (regulator oils), we combusted each of modern oxalic acid (OX-II, NIST SRM 4990C) and $^{14}C$-blank coal (Fisher Scientific, Waltham, MA, USA, S98807) with CuO oxidizer under vacuum in quartz tubes (Boutton et al. 1983). Tubes were smashed inside previously flushed and sealed jars by vigorous shaking. Gas was then transferred to bags and extracted on the vacuum line, and subsequent corrections for atmospheric contamination were performed by the W.M. Keck AMS facility.

The NSC ages were estimated by comparing $\Delta^{14}C$ to the annual plant record at Eight Mile Lake (EML) on the Bonanza Creek LTER near Healy, AK, USA (Ebert et al. 2017). The EML $\Delta^{14}C$ record compares extremely well with other northern hemisphere records (Figure S4 available as Supplementary data at *Tree Physiology* Online), and we used it to estimate an annual change in $\Delta^{14}C$ of −4‰ per year, representing an approximately linear decline over the past 16 years (Figure S4 available as Supplementary data at *Tree Physiology* Online). In early September 2018, to quantify the fossil fuel dilution of atmospheric $\Delta^{14}C$ at our sites, we collected respired $CO_2$ from leaves from each study tree. We created pooled samples by placing two leaves from each of the trees measured for $\Delta^{14}C$ at each site into a single jar from which gas was extracted for $\Delta^{14}C$ measurements as above, except incubations were done for 48 h. Respired $CO_2$ from pooled, late-season leaf samples, while not seasonally integrated, represents current-year photosynthate (Keel and Schädel 2010). We also measured bulk $\Delta^{14}C$ in *Helianthus annuus* (an annual plant) samples from nearby (<20 miles away from our sites), low-traffic roadsides. Mean $\Delta^{14}C$ of the two 2018 annual samples at EML was 5.7 ‰; overall mean $\Delta^{14}C$ of our pooled leaf respiration samples and *H. annuus* was also 5‰ (Figure S5 available as Supplementary data at *Tree Physiology* Online). A regional map of atmospheric $\Delta^{14}C$ also suggests that these two sites are unlikely to be strongly influenced by the regional population centers (Hsueh et al. 2007). Therefore, we did not adjust $\Delta^{14}C$ values for atmospheric differences between sites or from the EML record, and note that our analysis is focused on how trends across rings differ rather than absolute differences in the estimated age.

### *Statistical comparisons*

The NSC mean concentration comparisons were made using means estimated within a hierarchical Bayesian model accounting for ring depth (i.e., young, rings 1–6 vs old, rings 7–55) within trees within sites (Methods S2 available as Supplementary data at *Tree Physiology* Online). Such hierarchy draws mean parameter estimates for different depths within a tree closer together, which is somewhat akin to a repeated measures correction (Gelman et al. 2012). To compare total NSC pools calculated with Eqs (1) and (2), we simply summed (modeled) the mean concentrations across all rings within a tree, resulting in total NSC pools for five trees at each site; these satisfied the Shapiro test for normality, and total NSC pools at the two sites were subsequently compared with a *t*-test. For $\delta^{13}C$, because wet and dry sites appeared to be similar, we averaged all observations of either young or old rings across trees, then compared young and old rings across trees with a single paired *t*-test. Results of statistical tests were generally insensitive to the type of test used. To compare bark NSC concentrations across sites, we used a *t*-test on log-transformed values.

Finally, to evaluate if the trends in NSC age differ between sites, we also applied a random (i.e., tree-level) intercepts model for NSC age versus ring, $r$ (where $r = 1$ for rings formed in 2017, $r = 2$ for rings formed in 2016, etc.). We ignored pooling of multiple rings (e.g., we assumed $r = 2$, the midpoint, for a sample containing rings 1–3). We included squared terms for $r$ if significant. This model was fit in a Bayesian framework where for a given observation, $i$, of NSC age ('age') for tree, $t(i)$, at site, $s(i)$,

$$\text{Likelihood} : \text{age}_i \sim \text{Normal}\left(\mu_i, \sigma^2\right). \quad (3)$$

$$\text{Model} : \mu_i = \alpha_{1,t(i)} + \alpha_{2,s(i)} r_i + \alpha_{3,s(i)} r_i^2. \quad (4)$$

Thus, we assumed age was normally distributed with mean $\mu_i$ and variance $\sigma^2$, where the $\alpha$ terms are the regression parameters. These parameters, $\alpha$, were given diffuse normal priors, where $\alpha_1$ (i.e., intercepts) was modeled hierarchically around site-level means (see Methods S3, available as Supplementary data at *Tree Physiology* Online, for code). To understand the mean radial trends at each site, we define $\xi_i$ as the difference between the observed $\Delta^{14}C$ ages of NSC and their associated tree-level random intercepts ($\alpha_1$, tree-level NSC age at $r = 0$):

$$\xi_i = \text{age}_i - \alpha_{1,t(i)}. \quad (5)$$

We also assessed a number of more sophisticated linear and broken-stick models in a Bayesian framework, but these showed similar results to the simpler analysis above. For example, uncertainty in estimated effects introduced by variable RWs (i.e., 2017 ring is wider than 2016 ring), or AMS error did not influence the results (see Methods S4 available as Supplementary data at *Tree Physiology* Online). In general, we selected and interpreted the model with the best fit to the data as measured by the coefficient of determination ($R^2$). All statistics were performed in R (R Core Team 2022), and Bayesian models were implemented in JAGS 3.4.0 (Plummer 2003) using the package rjags (Plummer 2013). In reporting significance for parameters from Bayesian models, we report so-called Bayesian *P*-values based upon the posterior probability that the difference

between parameters is >0 (or that a given parameter is different from zero); we consider $P < 0.05$ as significant.

## Results

As reported below, NSC concentrations, isotopic values and pool sizes differ among the youngest six rings and older rings, particularly at the dry site. This young/old boundary aligns with the 2011–12 regional drought, and a transition between 'fast' and 'slow' pools around rings 5–8 is consistent with another study (e.g., Richardson et al. 2015). The RWs at the dry site are also particularly narrow in the years after this point (Table 1). Thus, we report results with respect to young (recent six rings, 2017–12) and old (deeper rings, 2011-heartwood boundary) pools, always as mean ± SD. Except for NSC ages inferred from $\Delta^{14}C$ (which increase with depth), results are generally insensitive to the chosen young/old boundary year. Bulk WD was 589 ± 20 kg per $m^3$ (dry site) and 463 ± 7 kg per $m^3$ (wet site). Total NSC concentration measured in previously incubated samples was 47% ± 25% ($n = 12$) lower compared with unincubated replicates; samples with total NSC concentrations >7 mg per g showed a concentration reduction of 60% ± 19% ($n = 9$) after incubation.

### *Non-structural carbohydrate concentrations*

Trees at the dry site generally exhibited higher sugar concentrations but lower starch concentrations than trees at the wet site (Figure 2a and b). Sugar concentrations and trends varied between sites. For example, sugar declined with sapwood depth at the dry site, but not at the wet site (Figure 2a). Starch concentrations and their radial trends did not significantly differ between sites, though spring starch concentrations in young rings at the dry site were extremely low (~0.25 mg per g). Thus, evidence spring dry-site starch was lower compared with fall was weak ($P = 0.11$) due to the low sample size and small concentrations in both seasons. Starch concentrations were higher at the wet site regardless of season (Figure 2b). In addition, while mean soluble sugar concentrations exceeded those of starch by 13 to 14 times at the dry site, they were only 2.8 (old rings) to 4.4 (young rings) times higher than starch concentrations for wet-site trees in sapwood and bark (Figure 2). Bark soluble sugar concentrations did not differ between sites (Figure 2c), but starch concentration was significantly higher at the wet site ($P < 0.05$, Figure 2d). The NSC concentrations at additional sites varied somewhat in accordance with aridity and were of similar magnitude as at the two focal sites (Figure S6 available as Supplementary data at *Tree Physiology* Online).

### *Total sapwood NSC pools*

Consistent with H1, dry-site sapwood total NSC pools at the end of the growing season (computed via Eq. (2)) were 33–40% of the wet-site totals (despite higher sugar concentrations), where

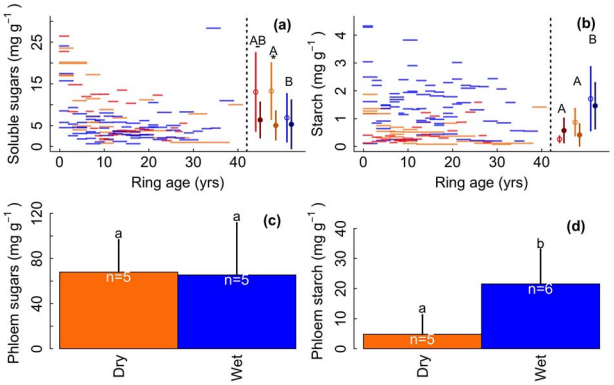


Figure 2. The NSC concentrations (mg per g dry mass) for (a, c) soluble sugars and (b, d) starch in glucose equivalents, measured in (a, b) sapwood rings and (c, d) bark (mean ± SD) at the wet (blue) and dry sites (spring sampling: red; fall sampling: orange). For sapwood (a, b), horizontal lines indicate rings that were pooled in a given sample (lines span ages of rings in sample), and circles to the right are means ± SD for young ($r = 1$–6, light red, orange, blue unfilled circles) and old ($r > 7$, dark red, orange, blue filled circles) rings. Statistical results are from a hierarchical Bayesian means model (Methods S2 available as Supplementary data at *Tree Physiology* Online), where uppercase letters denote significant differences among sites ($P < 0.05$), while '*' and '-' indicate that young and old ring means are significantly ($P < 0.05$) or marginally ($P < 0.06$) different, respectively, for a given site season. For bark (c, d), lowercase letters indicate the significant differences between wet and dry sites (*t*-test, $P < 0.05$). There was no spring sampling of bark at the dry site. See Table 2 for sampling dates; respiration rates are reported in supplement. The NSC data for other (secondary) sites are given in Figure S6 available as Supplementary data at *Tree Physiology* Online.

absolute differences between sites are much larger in older rings ($P < 0.05$, Figure 3). These totals ignore declining sample size into older rings, and those dry-site trees have shallower heartwood. However, summing by 6-year time periods (2011–06, 2005–2000, ..., 1981–76), cumulative NSC increases at a faster rate with increasing sapwood depth and reaches a higher maximum amount at the wet site than the dry site (Figure 3).

### *$\delta^{13}C$ of respired $CO_2$*

While $\delta^{13}C$ of respired $CO_2$ did not differ between sites, we found differences between young and old rings at both sites and between seasons at the dry site (Figure 4). In the fall at both sites, the mean $\delta^{13}C$ of respired $CO_2$ was significantly more negative (depleted)—indicating NSC fixed under relatively lower leaf water stress, or greater contribution from bark photosynthesis (Cernusak et al. 2001)—in young rings than old rings (Figure 4). In spring, $\delta^{13}C$ of $CO_2$ respired from young rings at the dry site was significantly less negative than that measured in fall (Figure 4), suggesting a higher degree of spring leaf water stress (Figure 4), as has been shown in another species in this region (Szejner et al. 2016, 2018), or lower contribution of bark photosynthesis, or discrimination during spring remobilization. These results indicate a change in mean $\delta^{13}C$ of respired $CO_2$

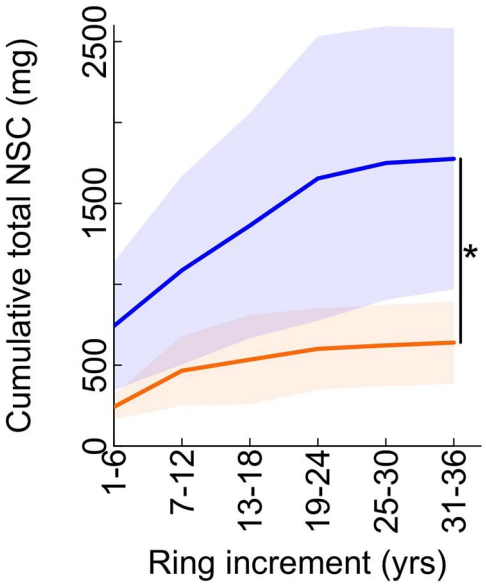


Figure 3. Cumulative total NSC (mean ± SD) across six ring increments, after accounting for differences in mean RW and WD (see Eqs (1) and (2)) at the wet (blue) and dry (orange) sites. Only fall NSC concentration data are used for the dry site. Shaded regions represent pool-wise means of 1000 among-tree ($n$ = 5 trees per site) SDs from replicate total NSC pool size calculations, which accounts for the analytical uncertainty estimated from repeat measurements of an in-house NSC standard, and 5% error in WD. Total NSC pools were significantly different ('*', $P < 0.05$, $t$-test). Total NSC pools here represent the NSC in a 1-cm thick bole section.

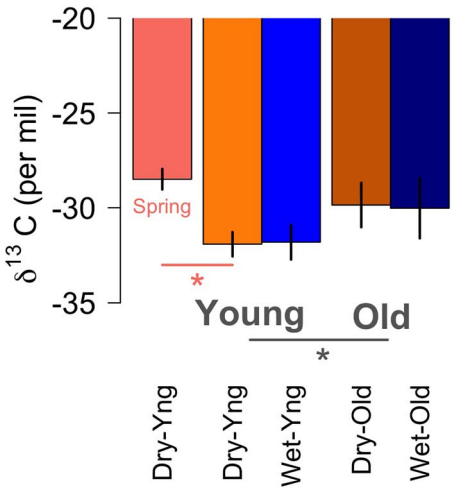


Figure 4. $\delta^{13}C$ (mean ± SD) of respired $CO_2$ at different depths (young or old rings) at both the dry (orange bars) and wet (blue bars) sites; $\delta^{13}C$ in young rings at the dry site during spring (pink bar) is also shown. The $\delta^{13}C$ was less negative in deeper pre-2012 ('Old') rings than in shallower post-2012 ('Yng') rings across both sites. In spring at the dry site, $\delta^{13}C$ was significantly less negative compared with the fall at the dry site. Spring sampling at the wet site was not possible (see Materials and methods). The $\delta^{13}C$ data for the other (secondary) sites are given in Table S2 available as Supplementary data at *Tree Physiology* Online. '*' indicates significant differences among seasons or depths ($P < 0.05$, paired t-test). Sites $\delta^{13}C$ were pooled together for young–old rings comparison.

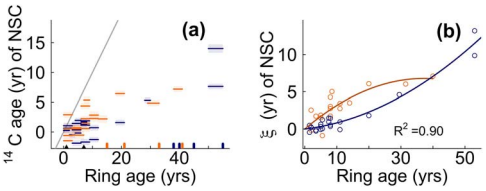


Figure 5. (a) The $\Delta^{14}C$ age of respired $CO_2$ and (b) $\xi$ of NSC ($\Delta^{14}C$ age after removing tree-level random intercepts), at dry (orange thin horizontal lines or circles) and wet (blue thin horizontal lines or circles) sites in aspen at the end of the growing season. In (a), colored horizontal lines span the ages of rings that were pooled into individual samples (see Figure 1), and reported AMS error is indicated by shading. The gray diagonal line is the 1:1 line, at which NSC age is exactly equal to ring age. Black triangles along the $x$-axis show timing of two recent El Niño events (2016 and 2009); orange (blue) dashes along the $x$-axis show heartwood boundaries for dry-site (wet-site) cores in which the boundaries were visually identifiable (four of five trees at each site). In (b), $\xi$ is equal to the $\Delta^{14}C$-derived ages after subtracting off the tree-level random intercepts (see Eq. (5)); showing opposite trends with depth at the wet and dry sites.

from the young ring NSC pool of ~3.5‰ at the dry site over the growing season (Figure 4), likely due to the influx of recently fixed NSC under less dry conditions post-monsoon onset.

### *Age of NSC pools inferred from $\Delta^{14}C$*

Bark NSC age was similar among sites (wet: 4.2 ± 2.1 years, $n$ = 6; dry: 4.3 ± 2.1 years, $n$ = 9). Ring-wise NSC age was younger than actual ring age, and this offset increased with sapwood depth at both sites (Figure 5a). In the oldest (deepest) rings measured, NSC age could be ~40 years younger than ring age, suggesting deep NSC mixing into old rings (full AMS dataset: Table S4 available as Supplementary data at *Tree Physiology* Online). The NSC ages in young rings were similarly young at both sites and were somewhat variable among trees within a site (Figure 5, Figure S7 available as Supplementary data at *Tree Physiology* Online), and so we focus primarily on the mean trends in NSC age (i.e., $\xi$, see Eq. (5)).

The model in Eqs (3) and (4) explained 90% of the variation in sapwood NSC ages, and quadratic terms were significant for both sites ($P < 0.05$), but of opposite sign ($P < 0.01$). In support of H2, we found that $\xi$—which removes among-tree variation at each site to allow for the inference on mean differences between sites (Eq. (5))—showed steeper initial increases in NSC age with depth at the dry site, which is consistent with H2. But this slope flattened in deeper tree rings due to a negative quadratic effect at the dry site compared with a positive quadratic effect at the wet site. That is, regression parameters ($\alpha_{2-3}$, Eq. (4)) both significantly differed between sites ($P < 0.01$), where the linear portion of the slope ($\alpha_2$) was significantly higher at the dry site (0.37 ± 0.11) compared with the wet site (0.05 ± 0.08), and the quadratic portion was negative (−0.005 ± 0.003) instead of positive (0.003 ± 0.001, Figure 5). Thus, while NSC aged gradually and then steeply

increased with depth at the wet site, the NSC age increased and then plateaued with depth at the dry site.

## Discussion

Site differences in the radial patterns of NSC pool size and age suggest that aridity and recent drought stress influence NSC utilization and mixing. While wet-site NSC ages match patterns from previous work where NSC becomes progressively, and then rapidly, older with depth (see Fig. 4a in Richardson et al. 2015), dry-site trees show significantly different radial patterns (Figure 5). In the south-western USA ('South-West'), trees experience dry conditions in June prior to monsoon arrival (Higgins et al. 1999), which creates a major seasonal stress that influences growth and NSC reserves (Peltier et al. 2020). During this period, both study sites experience similarly low mean precipitation conditions (mean June precipitation, wet site: 26.2 ± 24.7 mm, dry site: 21.7 ± 17.1 mm; Figure S2 available as Supplementary data at *Tree Physiology* Online). Differences between the NSC age of sites (Figure 5a and b) and total pool size in the fall (Figure 3) suggest that climate variation—namely moisture stress, as shown by the differences in tree physiological and growth traits between sites (Table 1 and Figure S1 available as Supplementary data at *Tree Physiology* Online)—limits the radial mixing of sapwood NSC. While we measured lower starch concentrations (Figure 2b) and smaller total NSC pools (Figure 3) at the dry site (supporting H1), we find mixed evidence for H2 (Figure 6a), where radial trends in NSC age differ (Figure 5); however, $\delta^{13}C$ suggests that mixing depth at both sites was similar in 2017, or at least was not extremely different (Figure 4). We thus propose a more complex conceptual model accounting for the inter-annual variability in NSC mixing, the role of varied mixing depth and potentially increased use (i.e., respiratory loss) of old NSC under moisture stress (Figure 6b).

Carbohydrate mixing in aspen growing in the South-West was relatively deep compared with other species and ecosystems (Carbone et al. 2013, Richardson et al. 2015, Trumbore et al. 2015). The oldest rings measured (1962–67) respired $CO_2$ only ~11–12 years old (Figure 5a). As the trees here are older compared with some studies, this could be an issue of ontogeny if allocation strategies change with age (Genet et al. 2009, Stephenson et al. 2014); however, deep reserves may become less accessible in larger trees if NSCs becomes permanently sequestered (Sala and Hoch 2009). Wood anatomy may also be related to the differences in mixing among species. Characterizations of NSC age by ring or sapwood depth are thus far limited to one pine species (*Pinus strobus*), red maple (*Acer rubrum*), *Sclerophyllum micranthum* and a few oak species (Carbone et al. 2013, Richardson et al. 2015, Trumbore et al. 2015). Two anatomical characteristics may restrict the generality of our results to other angiosperms: while aspen can form heartwood, anecdotally, the center of the bole is frequently affected by heartrot (Basham 1958) or partially disintegrated wood, suggesting that passive conversion of sapwood to heartwood (and loss of stored NSC) is possible. Relative to other species, aspen also has thick living bark (Figure S8 available as Supplementary data at *Tree Physiology* Online) that photosynthesizes (Cernusak et al. 2001) and supports high NSC concentrations (Figure 2c and d), but it is unclear how this may influence the radial NSC dynamics in sapwood.

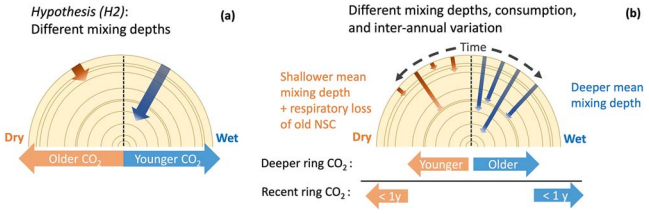


Figure 6. (a) We hypothesized (H2) that chronic aridity reduces surplus NSC and thus reduces the amount and depth of NSC mixed into sapwood, resulting in NSC ages that are more similar to ring ages (older) at the dry site compared with the wet site. (b) Our results, while consistent with H2 in shallow rings (steeper initial slope of NSC age at dry site), suggest NSC mixing depth varies across years and may also suggest greater reliance on old NSC at the dry site (younger deep ring NSC). A conceptual time series (years) of mixing depth at each site is illustrated: dry-site trees are chronically moisture limited, resulting in shallow mixing except in unusually wet years plus greater consumption; in contrast, NSC storage appears saturated at the wet site where mixing also appears relatively constant across years. Colored, inward pointing narrow arrows indicate NSC mixing depth; colored, outward pointing thick arrows indicate respired $CO_2$ (derived from NSC) and qualitative age. Arrows are colored according to site aridity (dry: orange; wet: blue).

### *H1: trees at drier sites store less NSC*

Lower total sapwood NSC, lower starch concentrations and seasonal NSC dynamics suggest that dry-site trees may store less stem NSC annually than wet-site trees (Figure 2b and Figure 3), which is consistent with H1. At the end of the growing season, dry-site trees store about one-third of the total NSC (for a given sapwood cross section) of wet-site trees. While spring and fall starch concentrations at the dry site did not differ (Figure 2b, $P = 0.11$), very low spring starch concentrations could suggest that dry-site trees may respire some starch in young rings to support metabolism during the pre-monsoon period (Figure 2b); sugars are likely maintained at high concentrations for osmoregulation (Guo et al. 2020, Peltier et al. 2020). As very little starch was present at the start of the growing season (Figure 2b, spring sampling), recently fixed NSC dominates the age signal of young rings in the dry-site trees (Figure 5a). However, wet-site young ring NSC age is also ~1 year old. Moreover, $\delta^{13}C$ in young and old rings was similar at both sites (Figure 4), which might suggest similar mixing depths in 2017. However, $\delta^{13}C$ could also be more negative in young rings because of mixing in of carbon from bark photosynthesis,

which also discriminates against $^{13}C$ (Cernusak et al. 2001, Cernusak 2020). But on average, wet-site trees likely store more and use proportionally less NSC, given deeper starch storage across rings (see Figure 2b and discussion below), with similar mass-specific respiration rates (Figure S9 available as Supplementary data at *Tree Physiology* Online), and higher maximum NSC ages (discussed below). Therefore, while we acknowledge we lack spring NSC observations at the wet site, $^{14}C$ ages suggest that wet-site trees contain a larger, deep sapwood NSC pool in the excess of annual respiratory costs and are well buffered from moisture variability.

### *H2: moisture stress influences NSC age and mixing*

While NSC age increases with depth in both sites, particularly in young rings, differences emerge in older deeper rings, where we suggest that radial patterns of NSC age at the dry site result from the moisture limitations on NSC mixing and perhaps higher consumption of old NSC. While mean NSC ages in young rings at the two sites are indistinguishable (<1 year), radial trends show that NSC age rises significantly faster with sapwood depth at the dry site (steeper initial slope, $\alpha_2$, Figure 5b). This is consistent with H2 (Figure 6a), where relatively shallower mixing of current photosynthate results in rapidly increasing NSC age with sapwood depth. At the wet site, gradually increasing NSC age with ring age (i.e., a relatively shallow slope, $\alpha_2$) is consistent with previous studies in more mesic forests (Carbone et al. 2013, Richardson et al. 2015). However, the radial pattern in dry-site NSC age differs in that the relationship between NSC age and ring age plateaus with depth (Figure 5b). That is, after rapid increases in NSC age for young rings, NSC age increases more slowly in deeper rings. We suggest this implies NSC mixing depth is also inter-annually variable, perhaps due to annual variation in the available photosynthate (Figure 6b).

Inter-annual variability in NSC mixing depths at the dry site could explain the plateauing of NSC age at the dry site (Figure 5), which is consistent with the current understanding of a passive component to NSC storage (Dietze et al. 2014). In moisture-limited dry-site trees, we suggest the occurrence of discrete 'mixing events' following favorable climate conditions, like the wet El Niño winter of 2015–16, which followed the drought of 2012 (Williams et al. 2013; noted on Figure 5). Higher NSC produced during favorable (wet) periods can mix (overflow) into deeper sapwood when demands of primary sinks (growth, respiration and osmotic regulation) and shallow sapwood storage are exceeded (e.g., Dietze et al. 2014, Hagedorn et al. 2016). This explains the juxtaposition of NSC age showing shallower past dry-site mixing (Figure 5b), but $\delta^{13}C$ suggesting similar 2017 mixing depth (spring vs fall sampling in Figure 4), and similar mean NSC ages in young rings across the two sites (Figures 5a and 6b). Similar climate conditions occurred in 2010–11 (El Niño) at both sites, when another 'mixing event' could have occurred. Stepped increases in age with sapwood depth, with shallower slope regions following favorable years, is only evident at the dry site, where climate is limiting to growth during recent years (Figure 6, Table 1; recent RWs 34% of wet-site mean). Episodic (or opportunistic) mixing of NSCs is consistent with highly variable regional climate with pronounced periodic cool- and warm-season precipitation extremes in the South-West (Griffin et al. 2013, Szejner et al. 2018, Peltier and Ogle 2019).

Alternative interpretations are possible and remain to be tested. Enhanced consumption (respiratory loss) of old NSC when deep mixing of young NSC is limited could also explain the apparent flattening of the slope where NSC age stops increasing with depth (Figure 5c). The dry site is also 1 °C warmer than the wet site, and temperature effects various physiological process, though the major effect of temperature is likely through its effect on vapor pressure deficit (Williams et al. 2013), as respiration processes have been shown to rapidly acclimate to increases in temperature (Rodríguez-Calcerrada et al. 2010). While not the focus of this study, tree-level variation suggests that non-climatic drivers of NSC dynamics could be important (Figure S7 available as Supplementary data at *Tree Physiology* Online). Dry-site trees could also be physiologically or morphologically adjusted to warmer or drier conditions: observed low growth could be adaptive if storage or osmotic control are prioritized (Galiano et al. 2017, Huang et al. 2019, Michelot-Antalik et al. 2019). Another morphological difference is that wet-site trees are larger (Table 1) and have thicker sapwood. Whether or not thick sapwood is maintained by higher NSC concentrations and deeper mixing, potentially of starch (Figure 2), is unknown. But, NSC is essential to the heartwood formation process, and thus critically low NSC could be one signal initiating active heartwood formation (Spicer 2005).

We argue that our conceptual framework (Figure 6b) also could explain high tree variability in the NSC ages: annual NSC availability may depend on unquantified physiological differences among trees. For example, certain dry-site trees showed evidence of past drought-related crown-dieback (Figure S1 available as Supplementary data at *Tree Physiology* Online), potentially limiting photosynthate production and mixing depth (e.g., Galiano et al. 2011). While crown dieback may confer future drought resistance by reducing leaf area (Martínez-Vilalta et al. 2009), dieback has been associated with reduced resilience to future drought in this species (Anderegg et al. 2013). As starch pools are nearly exhausted during the pre-monsoon arid period at the dry site, and replenished to lower levels than the wet site in the fall, we conclude that trees at the dry site are near their physiological limits and thus often have limited NSC except during unusually wet years. Another study using RWs from the same trees found that trees at the dry site tend to have shorter climate memory than trees at the wet site, that is, they are relatively more impacted by the growing season climate conditions (Peltier et al. 2021). Soluble sugar

patterns at both sites (Figure 2a), mirroring respiration rates (Figure S9 available as Supplementary data at *Tree Physiology* Online), could reflect osmotic requirements at the cellular level (Huang et al. 2019), with declining concentrations, with depth potentially reflecting the declining abundance of living parenchyma in older sapwood. It is also possible that deep NSC at the wet site could be unavailable (e.g., Sala et al. 2010), but there are few direct tests of this hypothesis (see Carbone et al. 2013). Other more mechanistic models could also be employed (Trumbore et al. 2015), but the assumption of such models of annually constant influx of NSC into storage does not seem to be supported by our data (Figure 5).

### *Comparison with other studies*

The NSC ages, here, are somewhat younger compared with the few studies of NSC ages and mixing via chemical extractions (e.g., Richardson et al. 2015). This difference is partly methodological as extractions have been shown to over-yield, potentially including some carbon that is not representative of reserves (i.e., not 'NSC', Peltier et al. 2023). It could also be possible that incubations are biased toward younger ages if young NSC is respired first. For example, following girdling in *S. micranthum* (Ducke), respired $CO_2$ age increased with time, showing that NSC was mobilized in reverse order of fixation (Muhr et al. 2018). The hypothesized mechanism of reverse chronological remobilization (Muhr et al. 2018) is spatially dependent such that deeper stores are harder to mobilize; this mechanism does not apply to incubations of sections of tree rings within a jar since all rings in the section directly respire $CO_2$ into the jar. And, indeed, time series samples of incubation $\Delta^{14}C$ showed little evidence for the strong dependence of $\Delta^{14}C$ on incubation time, suggesting these effects are minor in this species when few rings are included in a sample (Peltier et al. 2023). The deposition of starch into granules is known to be depositional (the 'onion model'; Tester et al. 2004) such that new starch is deposited onto the outside of existing granules. This could suggest that the oldest starch molecules are respired only if starch storage is completely exhausted, but we note that measured starch concentrations, here, were in fact extremely low during spring in dry-site trees (nearly exhausted, Figure 2b). Regular seasonal interconversion of sugars and starches to modify osmotic potential and freezing tolerance (Furze et al. 2018*b*) would also reduce the spatial heterogeneity of starch age within granules. We note that other studies provide evidence of substantial interconversion among different NSC pools, where the age of soluble and insoluble NSC fractions is essentially indistinguishable in multiple species (Richardson et al. 2015). Furthermore, here, pre- and post-incubation NSC concentrations showed that a large proportion of NSC had been respired, so our isotopic measurements are likely fairly representative of the NSC pool. Similar to Muhr et al. (2018) and Peltier et al. (2023), we found no evidence of cellulose decomposition, where the large differences between cellulose age (e.g., 55 years) and NSC age (e.g., 11 years) would strongly influence $\Delta^{14}C$ if decomposition had occurred.

## Conclusions

We found trees at a drier site showed younger NSC ages in deep sapwood, suggesting moisture limitation may limit the mixing of NSC into deep sapwood and result in greater respiratory loss of old NSC. While we acknowledge the limitations of this study—small $\Delta^{14}C$ sample sizes, few sampling periods, no moisture manipulations and potential local adaptation—it has generated novel hypotheses for future experiments. Our results are not unique to our two focal sites and are generally supported by the sampling we conducted at additional sites (Figure S6 available as Supplementary data at *Tree Physiology* Online). Given deep NSC mixing, future studies might ask: how available is deep NSC (30+ year old rings) and what is its functional role? Age measurements in other species suggest that old NSC is physiologically accessible under certain circumstances (Carbone et al. 2013, Muhr et al. 2018), and this NSC can be respired (Figure 5). Here, NSC mixing at a dry site is historically constrained, but unusually favorable climate conditions (such as in 2017) may result in deep mixing events. These results suggest that sapwood NSC age profiles may provide inference on drought resilience, where trees with younger NSC pools are more likely to be carbon-limited and less resilient to stress, particularly if the frequency of favorable climate events declines under climate change.

## Supplementary data

Supplementary data for this article are available at *Tree Physiology* Online.

## Acknowledgments

We thank Michael Bangs and Michelle Wilson for lab assistance, David Auty for WD measurements and the Ogle lab for feedback.

## Funding

This work was funded by a National Science Foundation-Division of Environmental Biology (NSF-DEB) Doctoral Dissertation Improvement Grant (#DEB-1702017) and a National Science Foundation-Advances in Biological Informatics (NSF-ABI) grant (DBI#1458867). Supporting data were obtained under NSF RAPID grant #1643245.

## Authors' contributions

D.M.P.P. and K.O. conceived the study. P.N. assisted with NSC pool measurements. G.K., C.E. and D.M.P.P. designed the

incubation method. C.E. conducted $CO_2$ purification and graphitization. T.S. and C.E. helped interpret radiocarbon data. P.N. cross-dated and measured RWs. D.M.P.P. conducted all other field and lab work. D.M.P.P. wrote the first draft of the manuscript. All authors contributed to the revisions.

## Data availability statement

All isotope data ($\delta^{13}C$ and $\Delta^{14}C$) are provided in the supplement along with the code for Bayesian models. All other data are available upon request.

## References


Adams HD, Germino MJ, Breshears DD, Barron-Gafford GA, Guardiola-Claramonte M, Zou CB, Huxman TE (2013) Nonstructural leaf carbohydrate dynamics of *Pinus edulis* during drought-induced tree mortality reveal role for carbon metabolism in mortality mechanism. New Phytol 197:1142–1151.

Adams HD, Zeppel MJ, Anderegg WR et al. (2017) A multi-species synthesis of physiological mechanisms in drought-induced tree mortality. Nat Ecol Evol 1:1285–1291.

Anderegg WR, Plavcová L, Anderegg LD, Hacke UG, Berry JA, Field CB (2013) Drought's legacy: multiyear hydraulic deterioration underlies widespread aspen forest die-off and portends increased future risk. Glob Chang Biol 19:1188–1196.

Anderegg WRL, Berry JA, Smith DD, Sperry JS, Anderegg LDL, Field CB (2012) The roles of hydraulic and carbon stress in a widespread climate-induced forest die-off. Proc Natl Acad Sci USA 109:233–237.

Barbaroux C, Bréda N (2002) Contrasting distribution and seasonal dynamics of carbohydrate reserves in stem wood of adult ring-porous sessile oak and diffuse-porous beech trees. Tree Physiol 22:1201–1210.

Basham JT (1958) Decay of trembling aspen. Can J Bot 36:491–505.

Bloemen J, Vergeynst LL, Overlaet-Michiels L, Steppe K (2016) How important is woody tissue photosynthesis in poplar during drought stress? Trees 30:63–72.

Boutton TW, Wong WW, Hachey DL, Lee LS, Cabrera MP, Klein PD (1983) Comparison of quartz and pyrex tubes for combustion of organic samples for stable carbon isotope analysis. Anal Chem 55:1832–1833.

Carbone MS, Czimczik CI, Keenan TF, Murakami PF, Pederson N, Schaberg PG, Xu X, Richardson AD (2013) Age, allocation and availability of nonstructural carbon in mature red maple trees. New Phytol 200:1145–1155.

Cernusak LA (2020) Gas exchange and water-use efficiency in plant canopies. Plant Biol 22:52–67.

Cernusak LA, Marshall JD, Comstock JP, Balster NJ (2001) Carbon isotope discrimination in photosynthetic bark. Oecologia 128: 24–35.

Chow PS, Landhäusser SM (2004) A method for routine measurements of total sugar and starch content in woody plant tissues. Tree Physiol 24:1129–1136.

Cole CT, Anderson JE, Lindroth RL, Waller DM (2010) Rising concentrations of atmospheric CO2 have increased growth in natural stands of quaking aspen (*Populus tremuloides*). Glob Chang Biol 16:2186–2197.

Dickman LT, Mcdowell NG, Sevanto S, Pangle RE, Pockman WT (2015) Carbohydrate dynamics and mortality in a piñon-juniper woodland under three future precipitation scenarios. Plant Cell Environ 38:729–739.

Dietze MC, Sala A, Carbone MS, Czimczik CI, Mantooth JA, Richardson AD, Vargas R (2014) Nonstructural carbon in woody plants. Annu Rev Plant Biol 65:667–687.

Ebert CH, Schuur EAG, Hicks-Pries CE (2017) Eight Mile Lake Research Watershed, Thaw Gradient, The radiocarbon value of ecosystem respiration, 2004–2016. Bonanza Creek LTER - University of Alaska Fairbanks. http://www.lter.uaf.edu/data/data-detail/id/515.

Ellison AM, Bank MS, Clinton BD et al. (2005) Loss of foundation species: consequences for the structure and dynamics of forested ecosystems. Front Ecol Environ 3:479–486.

Fritts HC, Swetnam TW (1989) Dendroecology: a tool for evaluating. Adv Ecol Res 19:111–188.

Furze ME, Huggett BA, Aubrecht DM, Stolz CD, Carbone MS, Richardson AD (2018*a*) Whole-tree nonstructural carbohydrate storage and seasonal dynamics in five temperate species. New Phytol 221:1466–1477.

Furze ME, Trumbore S, Hartmann H (2018*b*) Detours on the phloem sugar highway: stem carbon storage and remobilization. Curr Opin Plant Biol 43:89–95.

Galiano L, Martínez-Vilalta J, Lloret F (2011) Carbon reserves and canopy defoliation determine the recovery of Scots pine 4 yr after a drought episode. New Phytol 190:750–759.

Galiano L, Timofeeva G, Saurer M, Siegwolf R, Martínez-Vilalta J, Hommel R, Gessler A (2017) The fate of recently fixed carbon after drought release: towards unravelling C storage regulation in *Tilia platyphyllos* and *Pinus sylvestris*. Plant Cell Environ 40:1711–1724.

Gelman A, Hill J, Yajima M (2012) Why we (usually) don't have to worry about multiple comparisons. J Res Educ Effect 5:189–211.

Genet H, Bréda N, Dufrêne E (2009) Age-related variation in carbon allocation at tree and stand scales in beech (*Fagus sylvatica* L.) and sessile oak (*Quercus petraea* (Matt.) Liebl.) using a chronosequence approach. Tree Physiol 30:177–192.

Gillespie AJ (1999) Rationale for a national annual forest inventory program. J For 97:16–20.

Griffin D, Woodhouse CA, Meko DM, Stahle DW, Faulstich HL, Carrillo C, Touchan R, Castro CL, Leavitt SW (2013) North American monsoon precipitation reconstructed from tree-ring latewood. Geophys Res Lett 40:954–958.

Guo JS, Gear L, Hultine KR, Koch GW, Ogle K (2020) Non-structural carbohydrate dynamics associated with antecedent stem water potential and air temperature in a dominant desert shrub. Plant Cell Environ 43:1467–1483.

Hagedorn F, Joseph J, Peter M et al. (2016) Recovery of trees from drought depends on belowground sink control. Nat Plants 2:16111.

He W, Liu H, Qi Y, Liu F, Zhu X (2020) Patterns in nonstructural carbohydrate contents at the tree organ level in response to drought duration. Glob Chang Biol 26:3627–3638. https://doi.org/10.1111/gcb.15078.

Higgins RW, Chen Y, Douglas AV (1999) Interannual variability of the North American warm season precipitation regime. J Clim 12:653–680.

Hilman B, Muhr J, Helm J, Kuhlmann I, Schulze E-D, Trumbore S (2021) The size and the age of the metabolically active carbon in tree roots. Plant Cell Environ 44:2522–2535.

Hoch G, Richter A, Körner C (2003) Non-structural carbon compounds in temperate forest trees. Plant Cell Environ 26:1067–1081.

Holmes RL (1983) Computer-assisted quality control in tree-ring dating and measurement. Tree-Ring Bulletin, 43:69–78.

Hsueh DY, Krakauer NY, Randerson JT, Xu X, Trumbore SE, Southon JR (2007) Regional patterns of radiocarbon and fossil fuel-derived CO2 in surface air across North America. Geophys Res Lett 34:L02816.

Huang J, Hammerbacher A, Weinhold A et al. (2019) Eyes on the future – evidence for trade-offs between growth, storage and defense in Norway spruce. New Phytol 222:144–158.

Keel SG, Schädel C (2010) Expanding leaves of mature deciduous forest trees rapidly become autotrophic. Tree Physiol 30:1253–1259.
Kobe RK (1997) Carbohydrate allocation to storage as a basis of interspecific variation in sapling survivorship and growth. Oikos 80:226–233.
Landhäusser SM, Lieffers VJ (2003) Seasonal changes in carbohydrate reserves in mature northern *Populus tremuloides* clones. Trees 17:471–476.
Landhäusser SM, Chow PS, Dickman LT et al. (2018) Standardized protocols and procedures can precisely and accurately quantify non-structural carbohydrates. Tree Physiol 38:1764–1778.
Levin I, Kromer B (2004) The tropospheric 14CO2 level in mid latitudes of the northern hemisphere (1959-2003). Radiocarbon 46:1261–1271.
Lowe DC (1984) Preparation of graphite targets for radiocarbon dating by tandem accelarator mass spectrometer (TAMS). Int J Appl Radiat Isot 35:349–352.
Martínez-Vilalta J, Cochard H, Mencuccini M et al. (2009) Hydraulic adjustment of Scots pine across Europe. New Phytol 184:353–364.
Michelot-Antalik A, Granda E, Fresneau C, Damesin C (2019) Evidence of a seasonal trade-off between growth and starch storage in declining beeches: assessment through stem radial increment, non-structural carbohydrates and intra-ring $\delta$13C. Tree Physiol 39:831–844.
Muhr J, Trumbore S, Higuchi N, Kunert N (2018) Living on borrowed time–Amazonian trees use decade-old storage carbon to survive for months after complete stem girdling. New Phytol 220:111–120.
O'Brien MJ, Leuzinger S, Philipson CD, Tay J, Hector A (2014) Drought survival of tropical tree seedlings enhanced by non-structural carbohydrate levels. Nat Clim Chang 4:710–714.
Palacio S, Hoch G, Sala A, Körner C, Millard P (2014) Does carbon storage limit tree growth? New Phytol 201:1096–1100.
Pegoraro E, Mauritz M, Bracho R et al. (2019) Glucose addition increases the magnitude and decreases the age of soil respired carbon in a long-term permafrost incubation study. Soil Biol Biochem 129:201–211.
Peltier D, Guo J, Nguyen P et al. (2020) Temporal controls on crown nonstructural carbohydrates in southwestern US tree species. Tree Physiol 41:388–402.
Peltier D, Guo J, Nguyen P et al. (2021) Temperature memory and non-structural carbohydrates mediate legacies of a hot drought in trees across the southwestern US. Tree Physiol 42:71–85.
Peltier D, LeMoine J, Ebert C, Xu X, Ogle K, Richardson A, Carbone M (2023) An incubation method to determine the age of available nonstructural carbon in woody plant tissues. Tree Physiol. https://doi.org/10.1093/treephys/tpad015.
Peltier DM, Ogle K (2019) Legacies of La Niña: North American monsoon can rescue trees from winter drought. Glob Chang Biol 25:121–133.
Plummer M (2013) rjags: Bayesian graphical models using MCMC. R package version 3–10. Retrieved from http://CRAN.R-project.org/package=rjags.
Plummer M (2003) JAGS: A program for analysis of Bayesian graphical models using Gibbs sampling. In: Proceedings of the 3rd International Workshop on Distributed Statistical Computing. Vienna, Austria, p 125. http://www.ci.tuwien.ac.at/Conferences/DSC-2003/Drafts/Plummer.pdf (16 March 2015, date last accessed).
Quentin AG, Pinkard EA, Ryan MG et al. (2015) Non-structural carbohydrates in woody plants compared among laboratories. Tree Physiol 35:1146–1165.
R Core Team (2022) R: a language and environment for statistical computing. R Foundation for Statistical Computing Vienna, Austria, 2015.
Richardson AD, Carbone MS, Keenan TF, Czimczik CI, Hollinger DY, Murakami P, Schaberg PG, Xu X (2013) Seasonal dynamics and age of stemwood nonstructural carbohydrates in temperate forest trees. New Phytol 197:850–861.
Richardson AD, Carbone MS, Huggett BA, Furze ME, Czimczik CI, Walker JC, Xu X, Schaberg PG, Murakami P (2015) Distribution and mixing of old and new nonstructural carbon in two temperate trees. New Phytol 206:590–597.
Rodríguez-Calcerrada J, Atkin OK, Robson TM, Zaragoza-Castells J, Gil L, Aranda I (2010) Thermal acclimation of leaf dark respiration of beech seedlings experiencing summer drought in high and low light environments. Tree Physiol 30:214–224.
Sala A, Hoch G (2009) Height-related growth declines in ponderosa pine are not due to carbon limitation. Plant Cell Environ 32: 22–30.
Sala A, Piper F, Hoch G (2010) Physiological mechanisms of drought-induced tree mortality are far from being resolved. New Phytol 186:274–281.
Sala A, Woodruff DR, Meinzer FC (2012) Carbon dynamics in trees: Feast or famine? Tree Physiol 32:764–775.
Savi T, Casolo V, Luglio J, Bertuzzi S, Gullo MAL, Nardini A (2016) Species-specific reversal of stem xylem embolism after a prolonged drought correlates to endpoint concentration of soluble sugars. Plant Physiol Biochem 106:198–207.
Spicer R (2005) Senescence in secondary xylem: heartwood formation as an active developmental program. In: Holbrook NM, Zwieniecki MA, eds. Vascular transport in plants. Cambridge, MA, USA: Academic Press, pp 457–475.
Stephenson NL, Das AJ, Condit R et al. (2014) Rate of tree carbon accumulation increases continuously with tree size. Nature 507:90–93. http://www.nature.com/nature/journal/vaop/ncurrent/full/nature12914.html (23 January 2014, date last accessed).
Szejner P, Wright WE, Babst F, Belmecheri S, Trouet V, Leavitt SW, Ehleringer JR, Monson RK (2016) Latitudinal gradients in tree ring stable carbon and oxygen isotopes reveal differential climate influences of the North American monsoon system. J Geophys Res-Biogeosci 121:1978–1991.
Szejner P, Wright WE, Belmecheri S, Meko D, Leavitt SW, Ehleringer JR, Monson RK (2018) Disentangling seasonal and interannual legacies from inferred patterns of forest water and carbon cycling using tree-ring stable isotopes. Glob Chang Biol 24:5332–5347.
Tester RF, Karkalas J, Qi X (2004) Starch—composition, fine structure and architecture. J Cereal Sci 39:151–165.
Trugman AT, Detto M, Bartlett MK, Medvigy D, Anderegg WRL, Schwalm C, Schaffer B, Pacala SW (2018) Tree carbon allocation explains forest drought-kill and recovery patterns. Ecol Lett 21:1552–1560.
Trumbore S, Czimczik CI, Sierra CA, Muhr J, Xu X (2015) Non-structural carbon dynamics and allocation relate to growth rate and leaf habit in California oaks. Tree Physiol 35:1206–1222.
Vogel JS, Southon JR, Nelson DE, Brown TA (1984) Performance of catalytically condensed carbon for use in accelerator mass spectrometry. Nucl Instrum Methods Phys Res Sect B 5:289–293.
Weiss JL, Overpeck JT, Cole JE (2012) Warmer led to drier: dissecting the 2011 drought in the southern US. Southwest Climate Outlook 11:3–4.
Wiley E, King CM, Landhäusser SM (2019) Identifying the relevant carbohydrate storage pools available for remobilization in aspen roots. Tree Physiol 39:1109–1120.
Williams AP, Allen CD, Macalady AK et al. (2013) Temperature as a potent driver of regional forest drought stress and tree mortality. Nat Clim Chang 3:292–297. https://doi.org/10.1038/nclimate1693.
Yoshimura K, Saiki S-T, Yazaki K, Ogasa MY, Shirai M, Nakano T, Yoshimura J, Ishida A (2016) The dynamics of carbon stored in xylem sapwood to drought-induced hydraulic stress in mature trees. Sci Rep 6:24513.